

**Mechanical oscillations frozen on discrete levels by two optical driving fields**Bing He<sup>1,\*</sup>, Qing Lin<sup>2,\*</sup>, Miguel Orszag<sup>1,3</sup> and Min Xiao<sup>4</sup><sup>1</sup>*Center for Quantum Optics and Quantum Information, Universidad Mayor, Camino La Pirámide 5750, 8580000 Huechuraba, Santiago, Chile*<sup>2</sup>*Fujian Key Laboratory of Light Propagation and Transformation, College of Information Science and Engineering, Huaqiao University, Xiamen 361021, China*<sup>3</sup>*Instituto de Física, Pontificia Universidad Católica de Chile, Casilla 306, Santiago, Chile*<sup>4</sup>*Department of Physics, University of Arkansas, Fayetteville, Arkansas 72701, USA*

(Received 5 August 2019; accepted 1 July 2020; published 20 July 2020)

We report a synchronization phenomenon which is simulated with an optomechanical system driven by two equally strong fields with different frequencies. Once the frequencies of the driving fields are properly matched, the amplitude and phase of the mechanical oscillator coupled to the cavity field, together with its frequency spectrum, will be frozen on one of the determined trajectories like energy levels, and the phenomenon exists for the drive intensity beyond a threshold. Interestingly, the mechanical motion can become highly sensitive to its initial condition and the perturbations during the beginning period of dynamical evolution but, unlike the aperiodicity in chaotic motion, it will nonetheless evolve to one of those fixed trajectories in the end. The scenario may find applications in detecting tiny changes in the environment.

DOI: [10.1103/PhysRevA.102.011503](https://doi.org/10.1103/PhysRevA.102.011503)

Nonlinear systems under external drives or with mutual couplings are full of interesting phenomena. One category of them is dynamical synchronization [1–4], which has been studied since the time of Huygens [5]. The frequencies and phases of multiple oscillators can be synchronized under weak mutual interaction to exhibit the behaviors such as the coordinated flashes of fireflies [6] and the injection locking of a laser array to increase output power [7]. Synchronization is accompanied by mode locking. When it is synchronized by a periodic force of constant amplitude, a nonlinear oscillator will be locked to a number of frequencies known as the devil's staircase. A display of the phenomenon in real physical system is the voltage-current relation called Shapiro steps for a Josephson junction in an AC field [8,9]. Among the previously studied synchronization phenomena, mode locking usually refers to synchronizing the frequency of an oscillator with that of an external drive or its oscillation phase with those of the other oscillators coupled to it. One may ask a further question, whether the amplitude of an oscillator can also be locked to a number of fixed values at the same time. For example, by locking the amplitude  $A$  of a mechanical oscillation  $X_m(t) = A \sin(\omega_m t)$  with the frequency  $\omega_m$  to a series of discrete  $A_n$  ( $n \geq 1$ ), its energy  $\mathcal{E}_m(t) = \frac{1}{2}[X_m^2(t) + P_m^2(t)]$  determined by its displacement  $X_m(t)$  and momentum  $P_m(t)$  will be located on a number of levels as if its quantization were realized only by means of classical physics. For a macroscopic object it is counterintuitive to conceive of the possible existence of its discrete energy levels.

We show that energy levels like those mentioned above can be created for a macroscopic object through a process illustrated in Fig. 1(a), which can be experimentally im-

plemented by driving a cavity field pressurized on a mechanical oscillator with two fields with different frequencies. Previous research on similar doubly driven or bichromatic optomechanical systems included optomechanically induced transparency (see, e.g., [10–12]), optomechanical chaos (see, e.g., [13,14]), and mechanical squeezing (see, e.g., [15–17]). In all these previous studies the intensities of the two driving fields used must be unequal, usually with one of the driving fields much stronger than the other. Instead, the phenomena illustrated below should emerge under two drives with equal intensities. A general nonlinear dynamics due to two or more different external drives has not been fully explored thus far, except for the stochastic resonance phenomenon involving one noise drive [18,19]. We focus here on the phenomena due to one red detuned coherent drive ( $\omega_1 = \omega_c - \omega_m$ ) and one resonant coherent drive ( $\omega_2 = \omega_c$ ). If acting alone, the former achieves the cooling effect of reducing the mechanical fluctuation in a thermal environment [20]. The two drives work together to bring about a type of previously unknown synchronization to two coupled oscillators that model the system as in Fig. 1(a). The real-time evolution of the system toward the synchronization also exhibits previously unknown behaviors.

In terms of the two perpendicular quadratures  $X_c$  and  $P_c$  of the cavity field, together with the displacement  $X_m$  and momentum  $P_m$  of the mechanical oscillator, the dynamical equations of the system read (see [21] for the definitions of these dimensionless variables)

$$\begin{aligned}\dot{X}_c &= -\kappa X_c - \sqrt{2}gX_m P_c + \{\sqrt{2}[E_1 + \sqrt{\kappa}\xi_1(t)] \cos(\Delta_1 t) \\ &\quad + \sqrt{2}[E_2 + \sqrt{\kappa}\xi_2(t)] \cos(\Delta_2 t)\}, \\ \dot{P}_c &= -\kappa P_c + \sqrt{2}gX_m X_c + \{\sqrt{2}[E_1 + \sqrt{\kappa}\xi_1(t)] \sin(\Delta_1 t) \\ &\quad + \sqrt{2}[E_2 + \sqrt{\kappa}\xi_2(t)] \sin(\Delta_2 t)\},\end{aligned}$$

\*These authors contributed equally to this work.

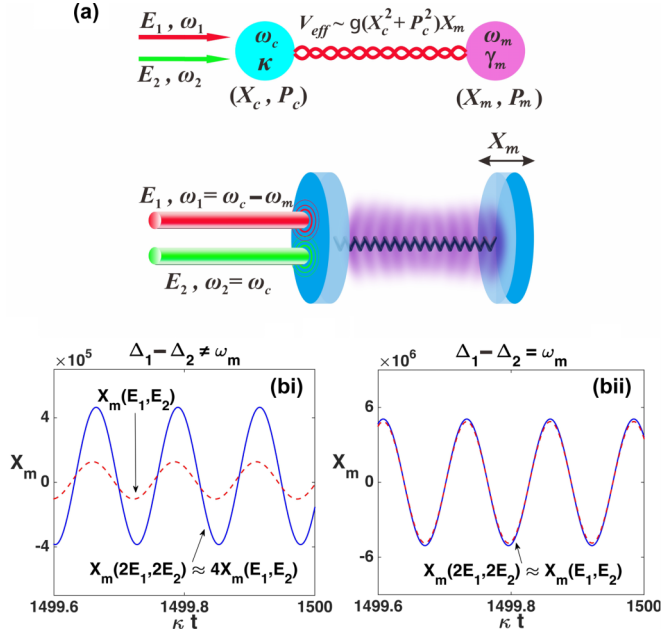


FIG. 1. (a) Setup of two drives on a cavity with a fixed mirror and a movable mirror (the mechanical oscillator) connected by a spring. This system exemplifies a general model of two oscillators with the intrinsic frequencies  $\omega_c$  and  $\omega_m$  and the damping rates  $\kappa$  and  $\gamma_m$  ( $\gamma_m \ll \kappa$  as in [20]), respectively. The radiation pressure of the cavity field modifies the cavity frequency  $\omega_c$  with a mechanical displacement  $X_m$  much less than the cavity length, realizing a nonlinear interaction potential  $V_{\text{eff}} \sim g(X_c^2 + P_c^2)X_m$  between the cavity field and mechanical oscillator. (b i) Stabilized  $X_m(t)$  linear responses to the increase of the drive amplitudes, when their frequencies do not match ( $\Delta_1 = 1.002\omega_m$  and  $\Delta_2 = 0$ ). (b ii)  $X_m(t)$  becomes frozen with the fixed  $A_1$  and  $\phi_1$ , once the condition  $\Delta_1 = \omega_m$  and  $\Delta_2 = 0$  is satisfied. Here we choose  $\omega_m = 50\kappa$ ,  $g = 10^{-5}\kappa$ , and  $\gamma_m = 10^{-5}\kappa$  for the system, as well as  $E_{1(2)} = 2.5 \times 10^5\kappa$ , and the existing noises are neglected.

$$\begin{aligned} \dot{X}_m &= \omega_m P_m, \\ \dot{P}_m &= -\omega_m X_m - \gamma_m P_m + \frac{1}{2}g(X_c^2 + P_c^2) + \sqrt{\gamma_m}\xi_m(t) \end{aligned} \quad (1)$$

in the observation system rotating at the cavity frequency  $\omega_c$ , where  $\Delta_{1(2)} = \omega_c - \omega_{1(2)}$  and the fluctuation  $\sqrt{\kappa}\xi_{1(2)}(t)$  of the drive amplitude  $E_{1(2)}$ , together with the mechanical noise  $\sqrt{\gamma_m}\xi_m(t)$  from the thermal environment, can exist. Any realistic system has a very small optomechanical coupling  $g$ . However, for such a driven system, the small nonlinear terms in Eq. (1) can govern the system dynamics. An example is shown in Fig. 1(b), where, given a small deviation from  $\Delta_1 = \omega_m$  and  $\Delta_2 = 0$ , the displacement  $X_m(t)$  responds linearly to the drive amplitude  $E$  (this notation stands for  $E_1 = E_2$ ), but the amplitude, frequency, and phase of the stabilized  $X_m(t)$  become frozen (no longer change with  $E$ ) under the condition  $\Delta_1 = \omega_m$  and  $\Delta_2 = 0$ .

Due to the resonance effect, only the sideband of mechanical frequency  $\omega_m$  amid the whole cavity field oscillation spectrum contributes to the mechanical motion significantly. Then any mechanical motion that has completely stabilized can be approximated as

$$X_m(t) = A \sin(\omega_m t + \phi) + d, \quad (2)$$

where  $A$  and  $d$  are the amplitude and pure displacement, respectively. In addition to the phenomenon illustrated in Fig. 1(b ii), where the mechanical oscillation amplitude  $A$  and phase  $\phi$  due to different external drive intensities are locked to the same values  $A_1$  and  $\phi_1$ , respectively, and they are frozen over a certain range of  $E$ , a still higher drive amplitude  $E$  can give rise to a series of such stabilized mechanical motion having the approximate energy

$$\mathcal{E}_m(t) = \frac{1}{2}A_n^2 + \frac{1}{2}d^2 + A_n d \sin(\omega_m t + \phi_n), \quad (3)$$

in which the displacement  $d$  is much less than the fixed oscillation amplitude  $A_n$  and the correspondingly locked phase  $\phi_n$  can be set equal to zero. Its time average  $\langle \mathcal{E}_m \rangle = \frac{1}{2}(A_n^2 + d^2) \approx \frac{1}{2}A_n^2$  is distributed on the quantized levels as in Fig. 2(a). Compared to the frozen amplitude  $A_n$ , the displacement  $d$  on each level slightly increases with  $E$ , leading to a certain width for the level.

Across the threshold drive amplitude around  $E \approx 5 \times 10^5\kappa$ , the illustrated system has completely reached the first level. Over a higher drive amplitude close to  $E \approx 2.5 \times 10^7\kappa$ , on the other hand, the second level emerges and seemingly overlaps with the first one. With the magnified scales in Fig. 2(b), the higher levels are found to still have a one-to-one correspondence between  $\langle \mathcal{E}_m \rangle$  and  $E$ . These discrete levels are not the common limit cycles like those of self-sustained oscillation (see, e.g., [24–27]), whose amplitudes can never be locked under a varying external drive.

The uniqueness of such discrete levels also exists in their oscillation patterns. The stabilized mechanical oscillations beyond the approximation in Eq. (2) can be found directly from the numerical simulations with Eq. (1) to have the stably oscillating mechanical energy as illustrated in Fig. 2(c). These numerically calculated patterns are dominated by the contours with the frequency  $\omega_m$  and amplitudes  $A_n d$ , being consistent with Eq. (3). Corresponding to each mechanical energy level, the stabilized cavity energy  $\mathcal{E}_c(t) = \frac{1}{2}[X_c^2(t) + P_c^2(t)]$  displays a fixed spectrum as one of the patterns in Fig. 2(d), though the amplitudes of the stabilized  $X_c(t)$  and  $P_c(t)$  are proportional to  $E$ . The level on which the mechanical oscillator is can thus be known from the corresponding cavity spectrum.

Under a given drive amplitude  $E$ , the mechanical oscillation matches the cavity oscillation spectrum in the form of  $n:m$  synchronization [2,4], where  $m$  and  $n$  are integers, as seen from the correspondence of the patterns in Figs. 2(c i)–2(c iv) to those in Figs. 2(d i)–2(d iv). The phase dynamics [28] is a primary concern in synchronization phenomena, including those in chaotic systems [29–33] and systems operating in a quantum regime [34–36]. A simultaneous phase locking on all entrained frequency components for the two oscillators that model the system as in Fig. 1(a), rather than on a couple of frequency components only, exists in the scenario with which we are currently concerned. Another fact about each discrete level is that all mechanical oscillations due to different drive amplitudes  $E$ , as well as their corresponding cavity oscillations, are also at the same pace.

The frozen mechanical motion must exist under one resonant field together with another equally strong cooling field. The functions of the two different driving fields can be found by starting only one of them and gradually strengthening the other (see [21]). A single resonant field with sufficiently

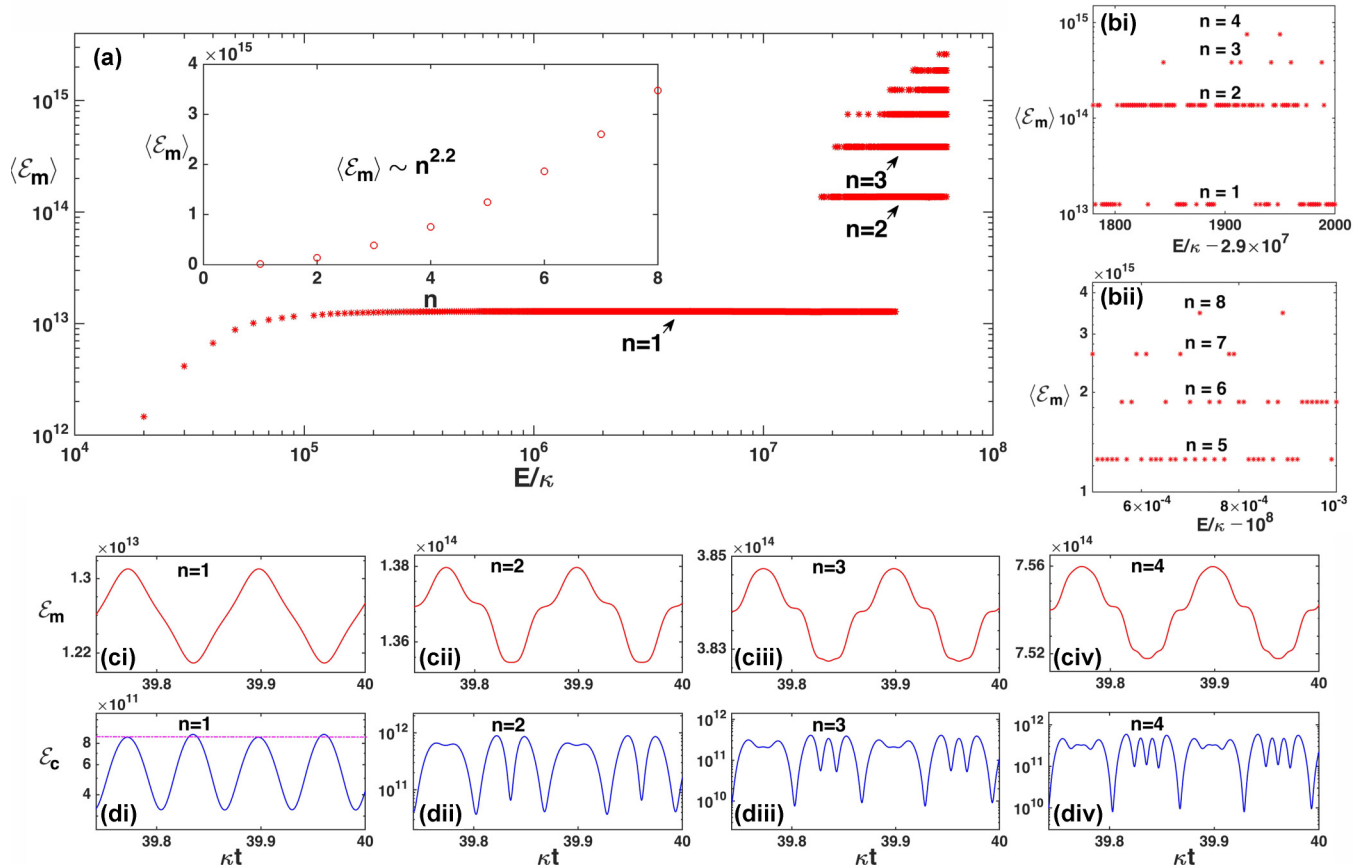


FIG. 2. (a) Relation of the average mechanical energy  $\langle \mathcal{E}_m \rangle = \frac{1}{2}(\langle X_m^2 \rangle + \langle P_m^2 \rangle)$  to the dimensionless drive amplitude up to  $E/\kappa = 6.3 \times 10^7$  (in terms of the logarithmic scales). The “quantized” mechanical energy on the displayed levels satisfies a power law  $\langle \mathcal{E}_m \rangle(n) \sim n^{2.2}$ , as shown in the inset. (b i) One section viewed with a scale on the order of  $10^3$ . (b2) View of another range starting from  $E/\kappa = 10^8$  with a scale of  $10^{-4}$  (the logarithmic scale on the vertical axis appears uneven). (c) and (d) One-to-one correspondence between the stabilized mechanical oscillations and cavity oscillations. The contours of  $\mathcal{E}_m(t)$  oscillating at the frequency  $\omega_m$  in (c) have their amplitudes  $A_n d$ , on the order of  $10^{-2}$  of the level positions  $\frac{1}{2}(A_n^2 + d^2)$ . In (d i) we use a dash line to make a single peak distinct.

high intensity brings about the discrete levels (the mechanical oscillation amplitude grows by discrete steps in response to increasing  $E$ ); the cooling field lowers the mechanical amplitude and locks the phase for all mechanical oscillations on each level. Their joint effect is to realize the discrete levels (the level  $n = 1$  is the top of the continuum spectrum) in Fig. 2(a) and the associated oscillation patterns such as those in Figs. 2(c) and 2(d).

The transient evolution processes will become complicated when the drive amplitude  $E$  is high enough to lead to the levels  $n \geq 2$ . As seen from Fig. 2(b), the system would go to another level whenever  $E$  is shifted to  $E + \delta E$  and the transition will occur with even less  $\delta E$  if  $E$  is still higher. When viewed with the scale used in Fig. 2(a), the different levels thus appear to overlap, being distinct from the step-by-step devil’s staircase [2,8] in other synchronization phenomena. Here the level transition means the evolution to a different level from the same initial condition rather than a direct jump between them. In this regime the average energy  $\langle \mathcal{E}_m \rangle$  is distributed irregularly along the axis of  $E$ , but its values are nonetheless fixed to those of the discrete levels.

Among the previously known phenomena, chaotic motion is typical in that a tiny change of initial condition will lead

to a huge difference in later evolutions. This characteristic also exists in our system when the drives are strong enough to create the higher levels. In Fig. 3 the evolution trajectories of  $\mathcal{E}_m(t)$ , which are determined by the corresponding  $X_m(t)$  and  $P_m(t)$ , are compared for some different initial variations  $\Delta \mathcal{E}_m(0) = \frac{1}{2}(\delta X_m^2(0) + \delta P_m^2(0))$ , where  $\delta X_m(0) [\delta P_m(0)]$  is the difference from the initial condition  $X_m(0) = 0 [P_m(0) = 0]$  only possible in a zero-temperature environment. Figure 3(a) displays the evolutions from different  $\delta X_m(0)$  on the order of  $10^{-6}$ , with one of the evolution courses being changed to another level. The dependence of an evolution course on its initial condition will become even more sensitive when the external drives are stronger. Figure 3(b) compares the evolution for the oscillator slightly touched at the beginning [ $\delta P_m(0) \sim 10^{-9}$ ] with the process without initial perturbation. Their initial difference is as small as  $\Delta \mathcal{E}_m(0) = 10^{-18}$ , but they finally arrive at two different levels separated by energy of a huge order  $10^{14}$ . Such sensitivity to the initial condition has nothing to do with chaos. There would be the tendency  $\lim_{t \rightarrow \infty} \Delta \mathcal{E}_m(t) / \Delta \mathcal{E}_m(0) \sim e^{\lambda t}$ , where  $\lambda$  is a positive Lyapunov exponent, were the mechanical oscillator in a chaotic motion. Instead, due to the limited energy influx from the two external drives, the actual tendency arising from difference

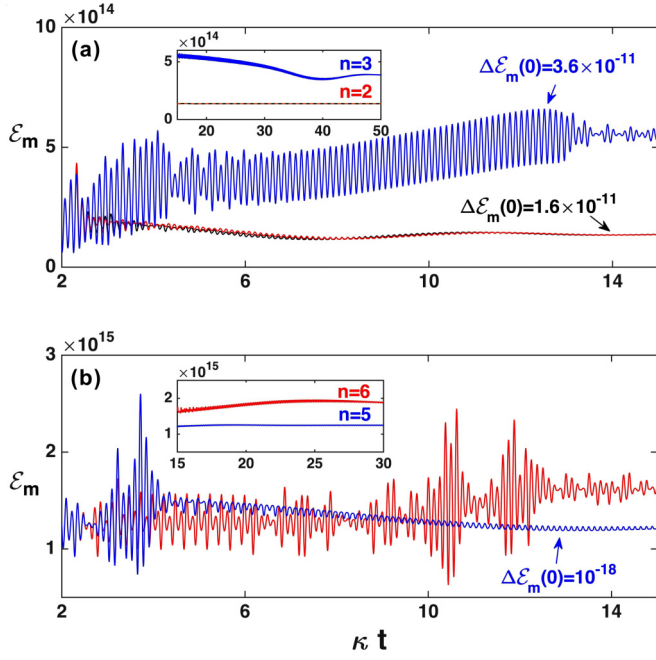


FIG. 3. (a) Evolutions under the fixed drives with  $E = 3.5 \times 10^7 \kappa$ , but with different initial conditions  $(X_m(0), P_m(0)) = (0, 0)$  for the red curve,  $(X_m(0), P_m(0)) = (4\sqrt{2} \times 10^{-6}, 0)$  for the black curve, and  $(X_m(0), P_m(0)) = (6\sqrt{2} \times 10^{-6}, 0)$  for the indigo curve. The inset shows the period of reaching the stability. (b) Evolutions of the mechanical energy under the fixed drives with  $E = (10^8 + 6.01 \times 10^{-4})\kappa$ , but with a tiny difference in the initial conditions:  $(X_m(0), P_m(0)) = (0, 0)$  for the red curve and  $(X_m(0), P_m(0)) = (0, \sqrt{2} \times 10^{-9})$  for the indigo curve. The mechanical oscillator may evolve to the level  $n = 7$  if its initial momentum reaches  $P_m(0) \sim 10^{-4}$ .

initial conditions is  $\lim_{t \rightarrow \infty} \Delta \mathcal{E}_m(t) / \Delta \mathcal{E}_m(0) \sim B \sin(\omega_m t) + D$ , where the constants  $B$  and  $D$  are bounded though they can be large. The system can have multiple attractors from varying initial conditions. However, once the system parameters ( $g/\kappa$ ,  $\omega_m/\kappa$ , and  $\gamma_m/\kappa$ ) are fixed, the oscillator will always evolve to one of those fixed levels as the attractors, no matter how the initial condition is modified.

Another important issue involves the noisy perturbations. One type of noise is the drive amplitude fluctuation  $\sqrt{\kappa} \xi_{1(2)}(t)$  in Eq. (1). First, we consider a small random fluctuation only on the cooling field [see Fig. 4(a)]. This fluctuation is added at two different moments, i.e., it carries a Heaviside function  $H(\kappa t - \kappa t_d)$  with different delay time  $t_d$ . The evolution of  $\mathcal{E}_m(t)$  after adding the fluctuation is compared with the ideally noiseless situation. It is found that a tiny random fluctuation added before the system reaches the stability will change the evolution course. However, if it acts when the system has been close to its stability, the same fluctuation cannot affect the evolution at all. In Fig. 4(b) much stronger fluctuations are added to both fields and similar consequences manifest as well. In an environment of high temperature, the thermal fluctuation  $\sqrt{\gamma_m} \xi_m(t)$  in Eq. (1) is not negligible and can be approximated as white noise [37]. We simulate the evolution under such mechanical noise in Fig. 4(c). The results are also similar to those of the drive fluctuations. The robustness of

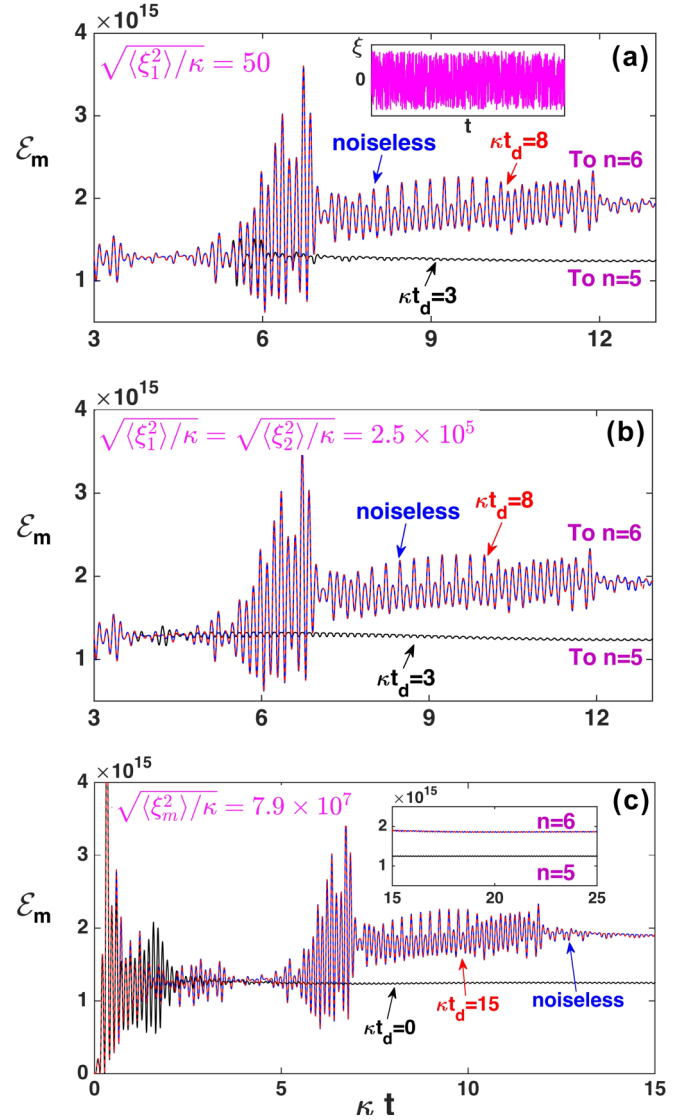


FIG. 4. (a) and (b) Influence on the evolution courses by the drive amplitude fluctuations in the form  $H(\kappa t - \kappa t_d) \xi_{1(2)}(t)$ , where  $\xi_{1(2)}(t)$  is a random function generated with MATLAB, as shown in the inset. The stochastic function changes its value for every step size of  $\kappa t = 1.5 \times 10^{-5}$ . The red curve due to the noisy perturbation added close to the stability almost coincides with the blue one (the evolution course exactly under  $E = 10^8 \kappa$  without any fluctuation). The black curve due to the perturbation added earlier evolves to another level. (c) Effect of a random drive  $H(\kappa t - \kappa t_d) \xi_m(t)$  on the mechanical oscillator. The noisy perturbation starting at the beginning ( $t_d = 0$ ) changes the evolution course (black curve), but the same noise acting much later will not affect the evolution (red curve).

the discrete energy levels against noisy perturbation allows their realization in a less demanding environment, though the evolution toward a specific level can be affected by the existing noises.

For a prepared system, the above-mentioned features manifest with increased drive intensity. The drive amplitude  $E$  used determines four different regimes as summarized in Fig. 5. A distinct boundary between these regimes does not exist, so the associated transitions are not like commonly known phase transitions. In addition to what has been discussed, this doubly

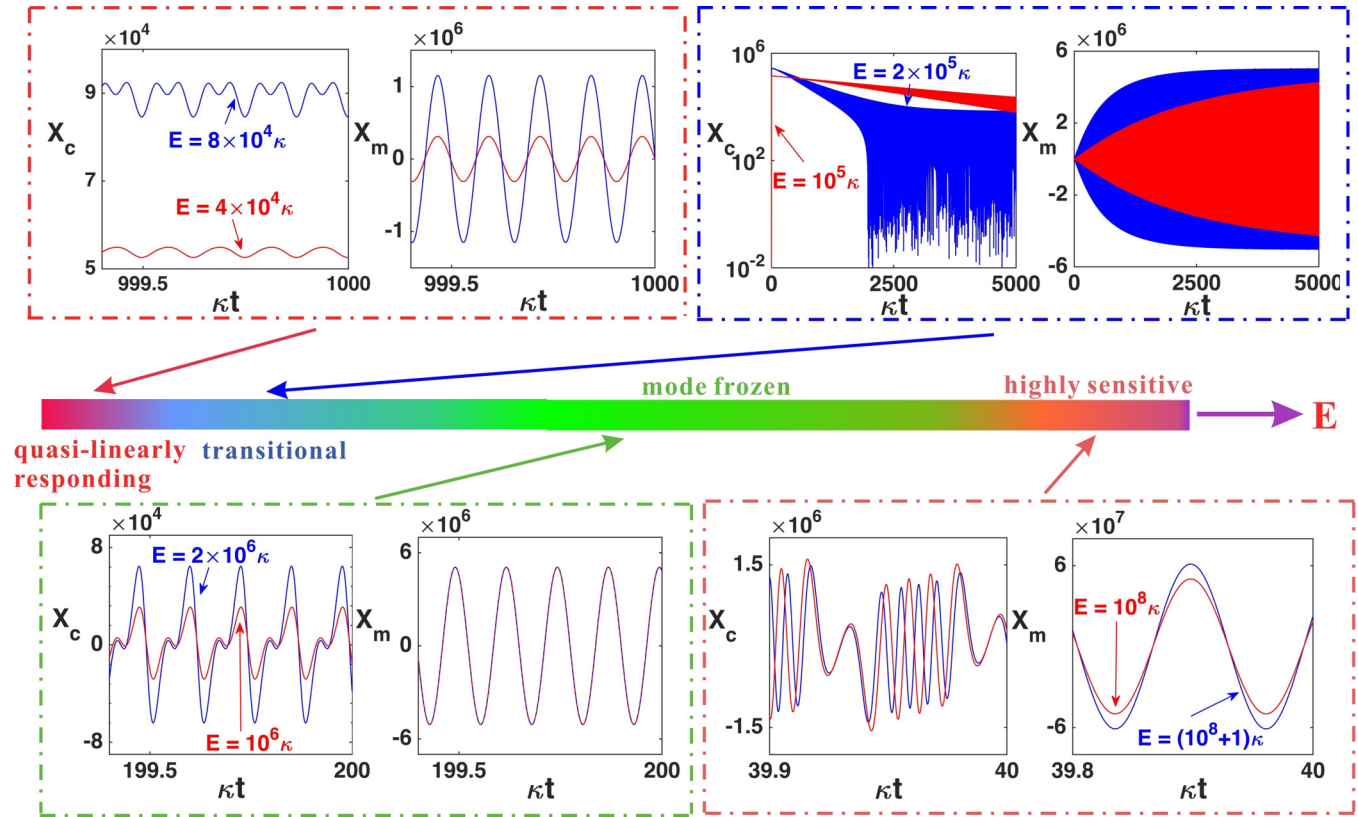


FIG. 5. Increasing drive amplitude  $E$  specifies the different dynamical regimes named after the corresponding mechanical responses. The illustrated  $X_c(t)$  and  $X_m(t)$  exemplify the associated dynamical behaviors. In the quasilinearly responding regime the amplitude of  $X_m(t)$  is proportional to  $E$ ; in the transitional regime both the cavity field and mechanical oscillator take a much longer time to reach stability; in the regime of mode locking (the level  $n = 1$ ),  $X_m(t)$  is frozen but  $X_c(t)$  becomes proportional to  $E$ ; in the highly sensitive regime a slight variation of  $E$  changes both the cavity and mechanical motion (the example shows a transition between  $n = 5$  and  $n = 6$ , as indicated by the peak numbers in a half period of cavity oscillation).

driven system displays an interesting behavior of a critical slowing-down when  $E$  is just less than required for the first level.

Our finding reveals the existence of a type of synchronization processes in which, unlike previously discovered synchronization phenomena, the three performance variables (amplitude, frequency, and phase) of an oscillator can be simultaneously locked. Such synchronization requires that the frequencies of the two external drives be rigorously matched, so it is possible to make use of this condition for the first mechanical level to measure the related physical quantities precisely. A transient evolution toward the higher

mechanical levels is sensitive to the initial condition and noisy perturbations, but the stabilized state is immune to the same perturbations. It is advantageous for the detection of tiny environmental changes, since the finally stabilized oscillations on the different discrete levels are distinguishable. The illustrated phenomena are expected to be observable with suitable optomechanical systems.

This work was sponsored by NSFC through Grant No. 11574093, a FONDECYT project through Grant No. 1180175, and Fondo de Iniciación, Universidad Mayor, Grant No. PEP I-2019021.

- [1] S. H. Strogatz and I. Stewart, Coupled oscillators and biological synchronization, *Sci. Am.* **269** (6), 102 (1993).
- [2] A. Pikovsky, M. Rosenblum, and J. Kurths, *Synchronization: A Universal Concept in Nonlinear Sciences* (Cambridge University Press, Cambridge, 2001).
- [3] R. V. Jensen, Synchronization of driven nonlinear oscillators, *Am. J. Phys.* **70**, 607 (2002).
- [4] A. Balanov, N. Janson, D. Postnov, and O. Sosnovtseva, *Synchronization: From Simple to Complex* (Springer, Berlin, 2009).

- [5] C. Huygens, *Horologium Oscillatorium* (Muguet, Paris, 1673).
- [6] J. Buck and E. Buck, Mechanism of rhythmic synchronous flashing of fire flies, *Science* **159**, 1319 (1968).
- [7] L. Goldberg, H. F. Taylor, and J. F. Weller, Injection locking of coupled-stripe diode laser arrays, *Appl. Phys. Lett.* **46**, 236 (1985).
- [8] S. Shapiro, Josephson Currents in Superconducting Tunneling: The Effect of Microwaves and Other Observations, *Phys. Rev. Lett.* **11**, 80 (1963).

- [9] A. K. Jain, K. K. Likharev, J. E. Lukens, and J. E. Sauvageau, Mutual phase-locking in Josephson junction arrays, *Phys. Rep.* **109**, 309 (1984).
- [10] G. S. Agarwal and S. Huang, Electromagnetically induced transparency in mechanical effects of light, *Phys. Rev. A* **81**, 041803(R) (2010).
- [11] S. Weis, R. Rivière, S. Deléglise, E. Gavartin, O. Arcizet, A. Schliesser, and T. J. Kippenberg, Optomechanically induced transparency, *Science* **330**, 1520 (2010).
- [12] A. H. Safavi-Naeini, T. P. M. Alegre, J. Chan, M. Eichenfield, M. Winger, Q. Lin, J. T. Hill, D. E. Chang, and O. Painter, Electromagnetically induced transparency and slow light with optomechanics, *Nature (London)* **472**, 69 (2011).
- [13] J. Ma, C. You, L. Si, H. Xiong, J. Li, X. Yang, and Y. Wu, Formation and manipulation of optomechanical chaos via a bichromatic driving, *Phys. Rev. A* **90**, 043839 (2014).
- [14] F. Monifi, J. Zhang, S.-K. Özdemir, B. Peng, Y.-X. Liu, F. Bo, F. Nori, and L. Yang, Optomechanically induced stochastic resonance and chaos transfer between optical fields, *Nat. Photon.* **10**, 399 (2016).
- [15] A. Kronwald, F. Marquardt, and A. A. Clerk, Arbitrarily large steady-state bosonic squeezing via dissipation, *Phys. Rev. A* **88**, 063833 (2013).
- [16] E. E. Wollman, C. U. Lei, A. J. Weinstein, J. Suh, A. Kronwald, F. Marquardt, A. A. Clerk, and K. C. Schwab, Quantum squeezing of motion in a mechanical resonator, *Science* **349**, 952 (2015).
- [17] J.-M. Pirkkalainen, E. Damskägg, M. Brandt, F. Massel, and M. A. Sillanpää, Squeezing of Quantum Noise of Motion in a Micromechanical Resonator, *Phys. Rev. Lett.* **115**, 243601 (2015).
- [18] L. Gammaitoni, P. Hänggi, P. Jung, and F. Marchesoni, Stochastic resonance, *Rev. Mod. Phys.* **70**, 223 (1998).
- [19] B. Lindner, J. Garcia-Ojalvo, A. Neiman, and L. Schimansky-Geier, Effects of noise in excitable systems, *Phys. Rep.* **392**, 321 (2004).
- [20] M. Aspelmeyer, T. J. Kippenberg, and F. Marquardt, Cavity optomechanics, *Rev. Mod. Phys.* **86**, 1391 (2014).
- [21] See Supplemental Material at <http://link.aps.org/supplemental/10.1103/PhysRevA.102.011503>, which contains Ref. [22] and Ref. [23], for a more detailed discussion.
- [22] W. Horsthemke and R. Lefever, *Noise-Induced Transitions* (Springer, Berlin, 2006).
- [23] B. He, L. Yang, Q. Lin, and M. Xiao, Radiation Pressure Cooling as a Quantum Dynamical Process, *Phys. Rev. Lett.* **118**, 233604 (2017).
- [24] T. Carmon, H. Rokhsari, L. Yang, T. J. Kippenberg, and K. J. Vahala, Temporal Behavior of Radiation-Pressure-Induced Vibrations of an Optical Microcavity Phonon Mode, *Phys. Rev. Lett.* **94**, 223902 (2005).
- [25] H. Rokhsari, T. Kippenberg, T. Carmon, and K. Vahala, Radiation-pressure-driven micro-mechanical oscillator, *Opt. Express* **13**, 5293 (2005).
- [26] F. Marquardt, J. G. E. Harris, and S. M. Girvin, Dynamical Multistability Induced by Radiation Pressure in High-Finesse Micromechanical Optical Cavities, *Phys. Rev. Lett.* **96**, 103901 (2006).
- [27] A. G. Krause, J. T. Hill, M. Ludwig, A. H. Safavi-Naeini, J. Chan, F. Marquardt, and O. Painter, Nonlinear Radiation Pressure Dynamics in an Optomechanical Crystal, *Phys. Rev. Lett.* **115**, 233601 (2015).
- [28] Y. Kuramoto, *Chemical Oscillations, Waves, and Turbulence* (Springer, Berlin, 1984).
- [29] V. S. Afraimovich, N. N. Verichev, and M. I. Rabinovich, Stochastic synchronization of oscillations in dissipative systems, *Radiophys. Quantum Electron.* **29**, 795 (1986).
- [30] L. M. Pecora and T. L. Carroll, Synchronization in Chaotic Systems, *Phys. Rev. Lett.* **64**, 821 (1990).
- [31] M. G. Rosenblum, A. S. Pikovsky, and J. Kurths, Phase Synchronization of Chaotic Oscillators, *Phys. Rev. Lett.* **76**, 1804 (1996).
- [32] J. M. González-Miranda, *Synchronization and Control of Chaos: An Introduction for Scientists and Engineers* (Imperial College Press, London, 2004).
- [33] N. Yang, A. Miranowicz, Y.-C. Liu, K. Xia, and F. Nori, Chaotic synchronization of two optical cavity modes in optomechanical systems, *Sci. Rep.* **9**, 15874 (2019).
- [34] T. E. Lee and H. R. Sadeghpour, Quantum Synchronization of Quantum van der Pol Oscillators with Trapped Ions, *Phys. Rev. Lett.* **111**, 234101 (2013).
- [35] S. Walter, A. Nunnenkamp, and C. Bruder, Quantum Synchronization of a Driven Self-Sustained Oscillator, *Phys. Rev. Lett.* **112**, 094102 (2014).
- [36] A. Roulet and C. Bruder, Synchronizing the Smallest Possible System, *Phys. Rev. Lett.* **121**, 053601 (2018).
- [37] Q. Lin, B. He, and M. Xiao, Entangling Two Macroscopic Mechanical Resonators at High Temperature, *Phys. Rev. Appl.* **13**, 034030 (2020).